Electronic Supplementary Information (ESI)

Theoretical Study on Propane Dehydrogenation Reaction Over Pt_xSn_y Intermetallic Compounds

Dan-Ni Chen,[†a] Chen-Xu Hu,[†a] Hao Lu,[a] Yao Jie,[a] Yi-Fan Zhang,[a] Jing-Yi Guo,[b] and Hong Yan[*a]

[a] *State Key Laboratory of Chemical Resource Engineering, College of Chemistry, Beijing University of Chemical Technology, Beijing 100029, China*

[b] *School of Engineering, Qinghai Institute of Technology, Xining, Qinghai, 810000, PR China*

* Corresponding Author:

yanhong@mail.buct.edu.cn (Hong Yan).

Contents

1. The structures of Pt(111), Pt_3Sn(111), Pt_1Sn_1(110) and Pt_2Sn_3(110) unit cells.

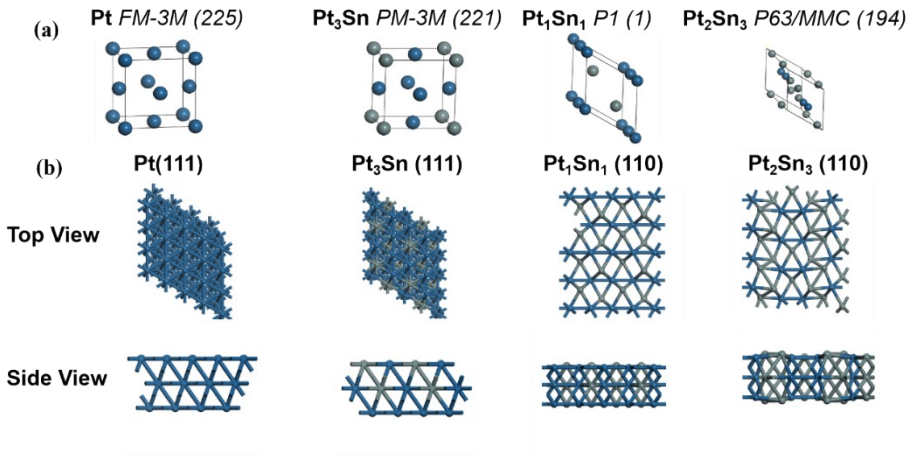

Figure S1. (a) Structural models of Pt, Pt_3Sn, Pt_1Sn_1 and Pt_2Sn_3 protocells; (b) top and side views of Pt(111) , Pt_3Sn(111) , Pt_1Sn_1(110) and Pt_2Sn_3(110) after optimization of the crystal surface structure

Table S1. Adsorption energies of intermediates on different supercells vary.

	supercells vary	E_{ads} / eV			
		C_3H_8*	C_3H_7*	C_3H_6*	$CH_3CH_2CH_2$*+H*
Pt(111)	p(1×2)	–0.654	–2.651	–1.985	–4.747
	p(2×2)	–0.644	–2.642	–1.995	–4.799
Pt_3Sn(111)	p(1×2)	–0.414	–1.775	–1.162	–4.364
	p(2×2)	–0.418	–1.773	–1.165	–4.373
Pt_1Sn_1(110)	p(2×2)	–0.460	–1.700	–0.651	–3.991
	p(2×4)	–0.457	–1.731	–0.843	–4.033
Pt_2Sn_3(110)	p(1×2)	–0.261	–2.226	–0.589	–3.337
	p(2×2)	–0.262	–2.229	–0.590	–3.393

2. The calculation of the surface energy.

Surface energy (SE) is defined as the amount of energy required to cleave an infinite crystal into two parts, i.e. the energy required to form a new surface. It is calculated as shown in eq2:

$$E_{surf} = \frac{1}{2A}(E_{slab} - E_{bulk})$$

Here, E_{slab} is the total energy of the slab, E_{bulk} is the energy in the bulk.

In general, it is known that the smaller the surface energy is, the easier is to form a surface, i.e., the surface with smaller surface energy is easier to be exposed. Therefore, according to the calculations, the most exposed crystal surface of Pt_2Sn_3 is (110)

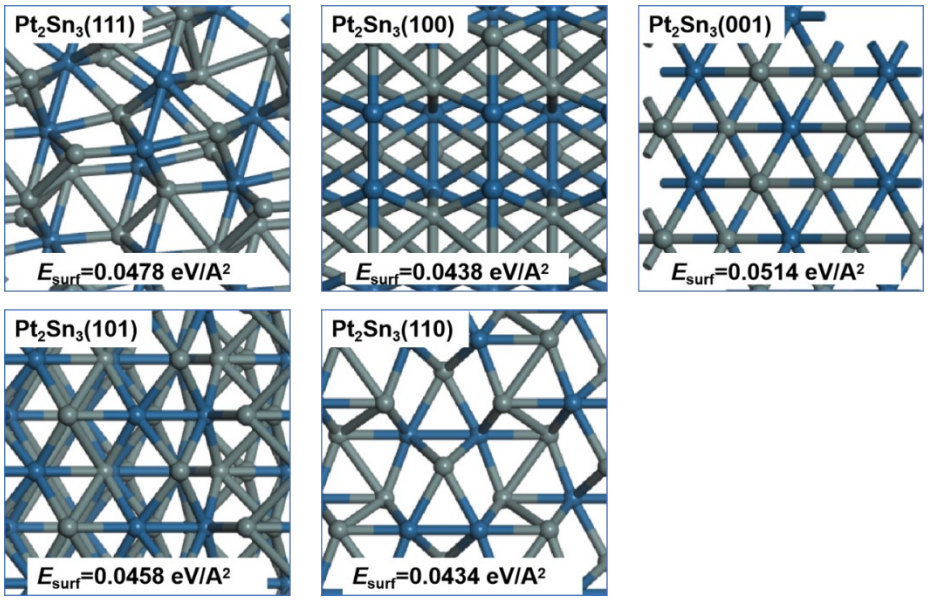

Figure S2. Top view of the optimized structure and surface energies (E_{surf}) of each surface of Pt_2Sn_3 (Pt: blue; Sn: grey)

3. Energy test for cut-off energy (ENCUT).

In order to make reasonable use of computing resources, we test the cut-off energy (ENCUT) required for the calculation. If the ENCUT is too small, the system will be difficult to converge, and if it is too large, it will take longer to waste computing resources. As shown in Figure S3, for the system we want to study, when the ENCUT is 400 eV, it can not only ensure the convergence of the system, but also save computing resources.

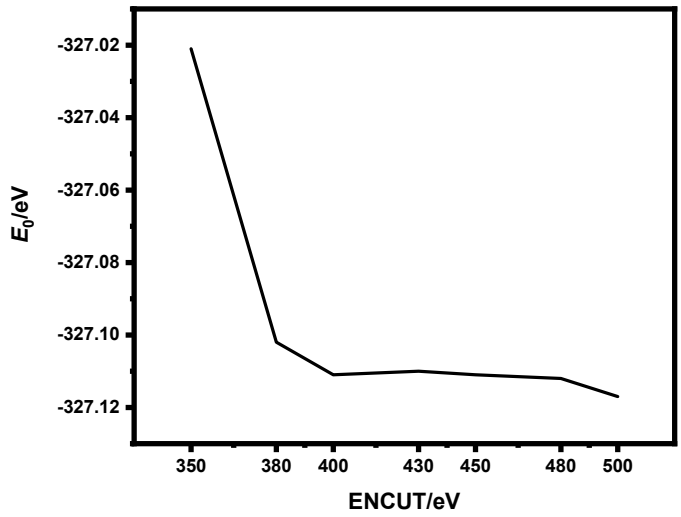

Figure S3. Take the energy E_0 of C_3H_8 adsorbed on Pt(111) surface as an example for ENCUT test.

4. Energy test for *k*-point.

As shown in Table S2, when the K-point is set to 3×3×1, the adsorption energy is –0.119 eV, and when the *k*-point is increased to 5×5×1, the DFT calculation results show that the adsorption energy has only a small change (0.004 eV). Therefore, in order to save computing resources, the *k*-point of 3×3×1 is used to complete all calculations.

Table S2. Adsorption energy of propane molecules on Pt(111) surface when *k*-point are 1×1×1, 3×3×1 and 5×5×1. (Unit: eV)

K-point	$E_{surface}$	$E_{adsorbate}$	$E_{adsorbate/surface}$	E_{ads}
1×1×1	–247.710	–57.087	–305.035	–0.238
3×3×1	–246.760	–57.011	–303.890	–0.119
5×5×1	–246.789	–57.010	–303.914	–0.115

5. Energy test for slab-thickness.

As shown in Table S3, the adsorption energies change subtly when the number of slabs larger than 3, suggesting that three-layer slabs are thick enough to represent the bulk structure. On the other hand, for the 3-layered structures, the energy difference between the bottom-layer fixed models and the full-relaxed ones on the same surface are slightly. Thus, in order to save the computational cost, the bottom-layer-fixed 3-layered models are used in this work.

Table S3. Calculated tests of 3L and 4L adsorption energies for Pt(111), Pt_3Sn(111), Pt_1Sn_1(110) and Pt_2Sn_3(110) surface plate models.

Energy/eV	3L		4L	
	Bottom-layer fixed	Full relaxed	Bottom-layer fixed	Full relaxed
E_{C3H8}	–57.011	–57.011	–57.011	–57.011
E_{slab}	–270.044	–270.044	–368.244	–368.244

E_{tol}	–327.125	–327.123	–425.315	–425.312
E_{ads}	–0.07	0.068	–0.06	0.057

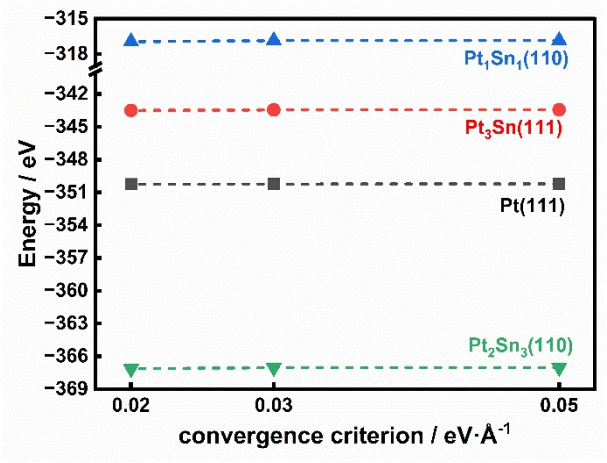

Figure S4. The energy for the convergence criterion test.

6. Adsorption site test.

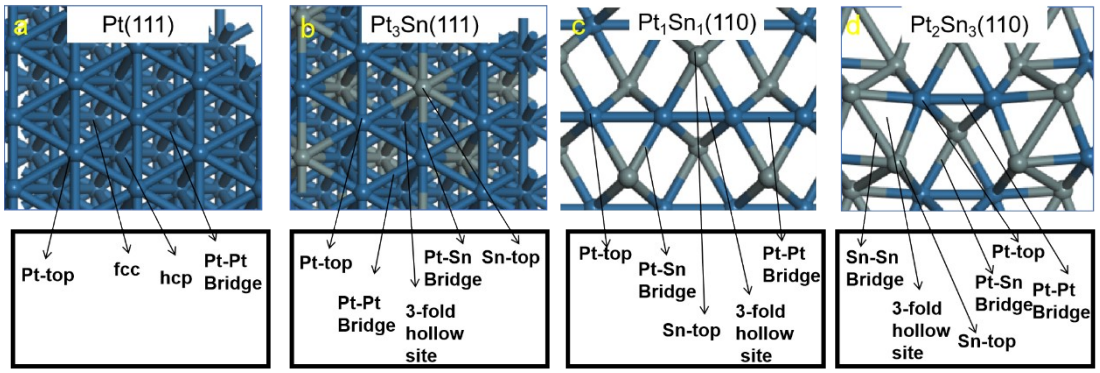

Figure S5. Different adsorption sites on Pt(111), $Pt_3Sn(111)$, $Pt_1Sn_1(110)$ and $Pt_2Sn_3(110)$.

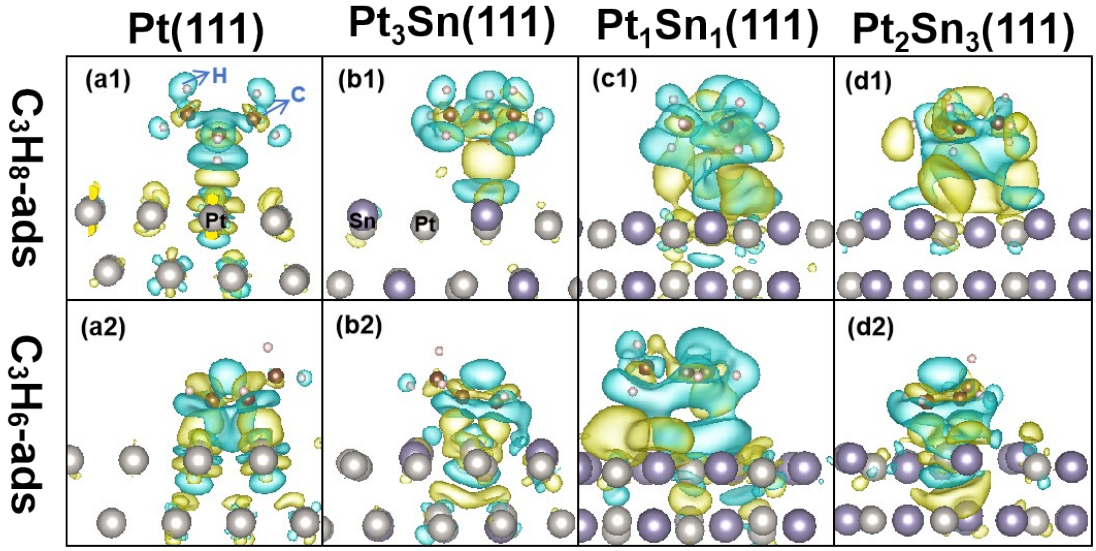

Figure S6. Calculated electron density difference diagrams of C_3H_8 and C_3H_6 adsorption on Pt(111), $Pt_3Sn(111)$, $Pt_1Sn_1(110)$ and $Pt_2Sn_3(110)$. Yellow represents an electron accumulation region and blue represents an electron loss region.

Several possible adsorption sites were tested in order to find the most stable adsorption sites for the products on the Pt(111), $Pt_3Sn(111)$, $Pt_1Sn_1(110)$ and $Pt_2Sn_3(110)$surfaces. The top and side views of the most stable adsorption sites and adsorption energies of the intermediates are shown in Figures S7-S12, and the relevant data are summarized in Table S4.

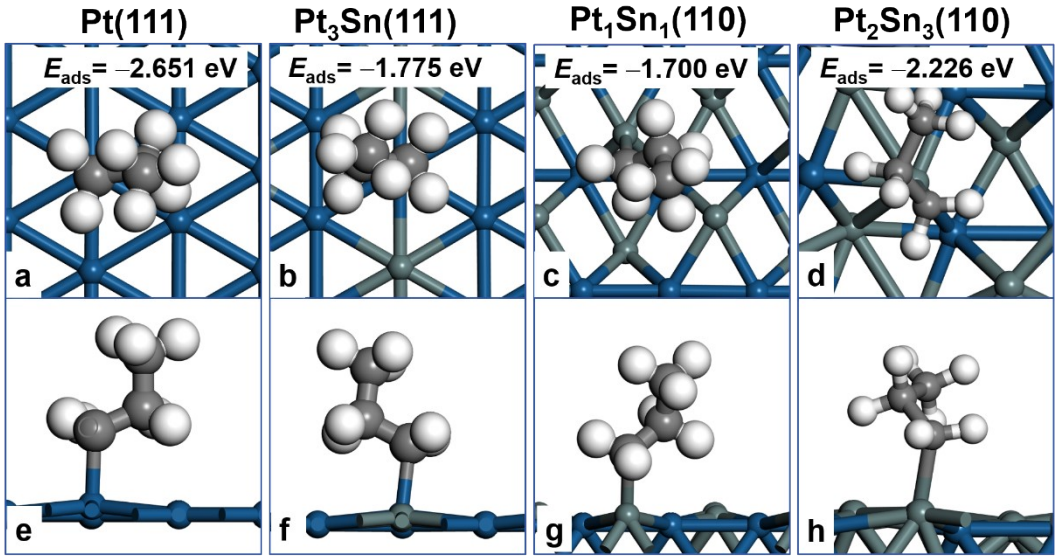

Figure S7. Top view (a-d) and side view (e-h) of the adsorption structures of 1-propyl on Pt (111), Pt_3Sn (111), Pt_1Sn_1 (110) and Pt_2Sn_3 (110). Pt: blue, Sn: grey, C: black, H: white

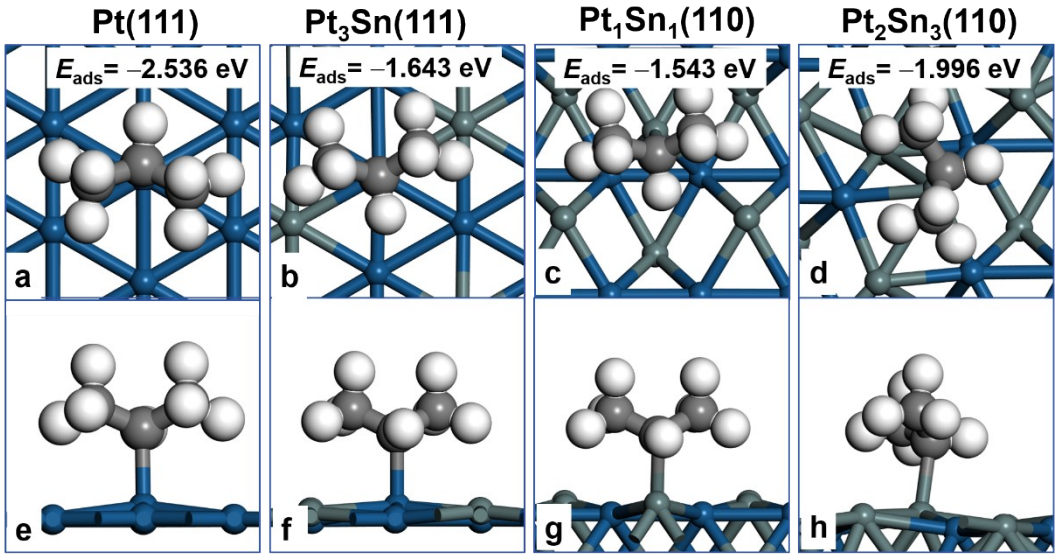

Figure S8. Top view (a-d) and side view (e-h) of the adsorption structures of 2-propyl on Pt (111), Pt_3Sn (111), Pt_1Sn_1 (110) and Pt_2Sn_3 (110). Pt: blue, Sn: grey, C: black, H: white

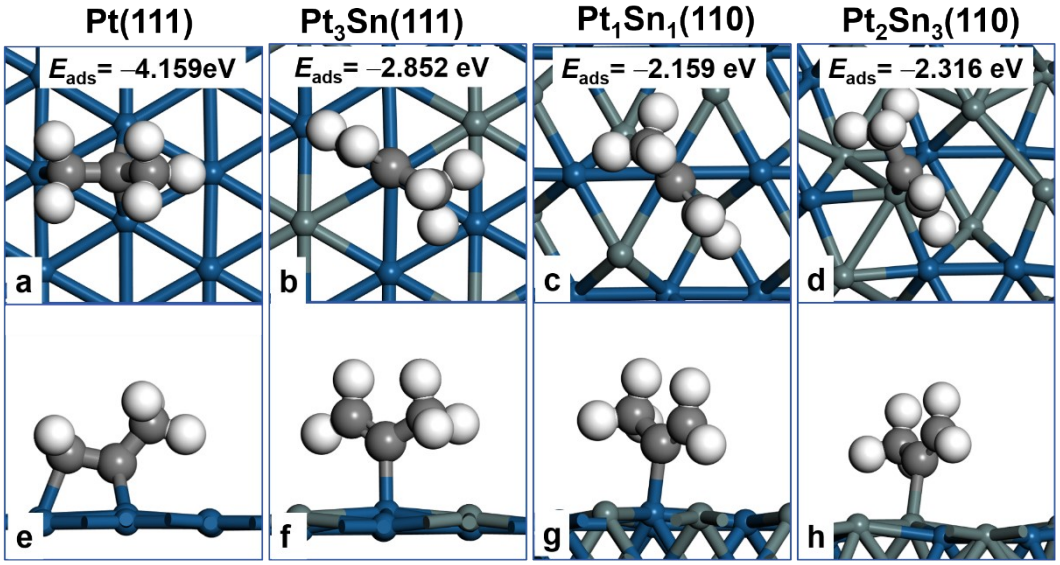

Figure S9. Top view (a-d) and side view (e-h) of the adsorption structures of CH_3CCH_2* on Pt(111), Pt_3Sn (111), Pt_1Sn_1 (110) and Pt_2Sn_3 (110). Pt: blue, Sn: grey, C: black, H: white

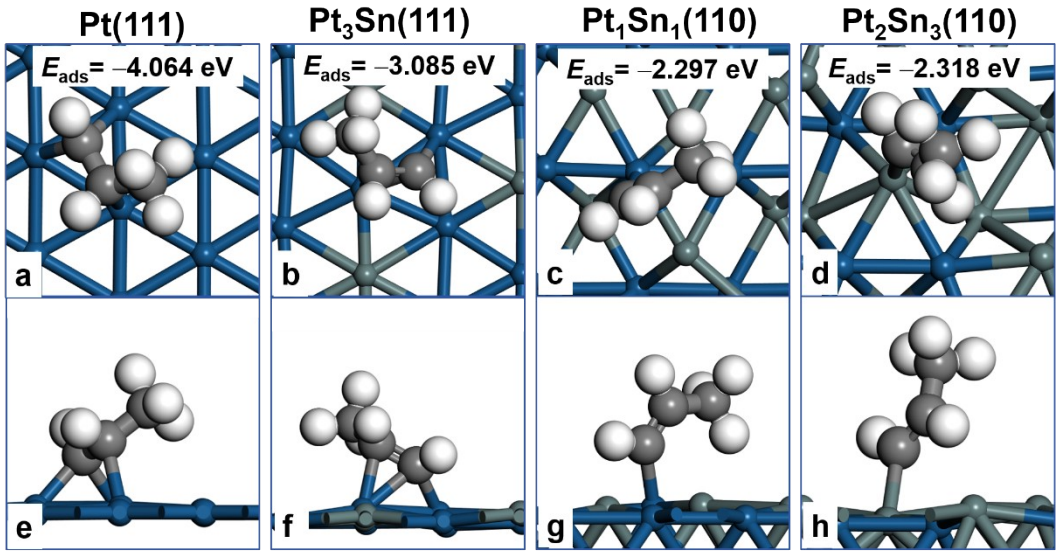

Figure S10. Top view (a-d) and side view (e-h) of the adsorption structures of CH_3CHCH* on Pt (111), Pt_3Sn (111), Pt_1Sn_1 (110) and Pt_2Sn_3 (110). Pt: blue, Sn: grey, C: black, H: white

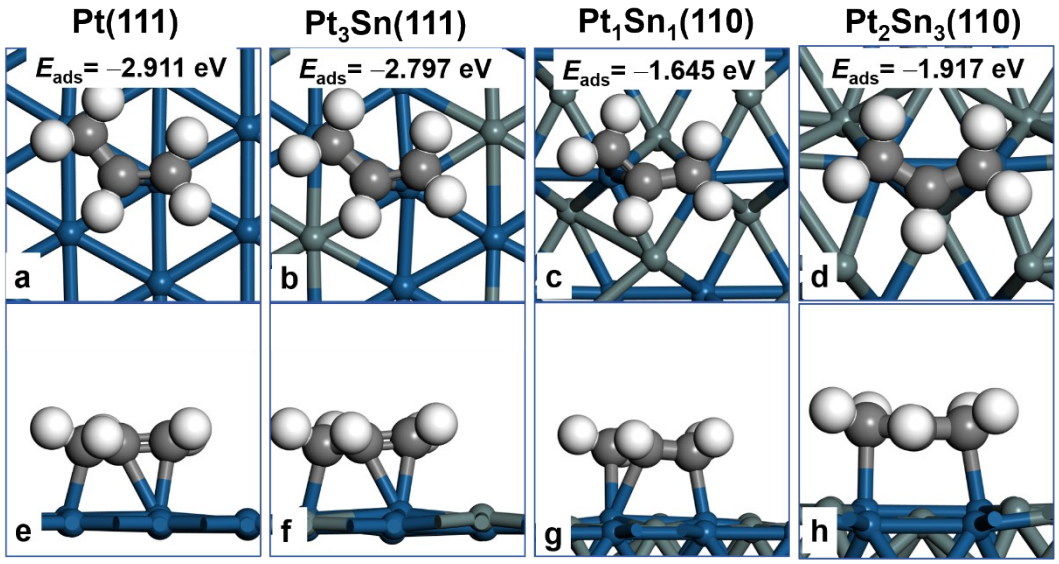

Figure S11. Top view (a-d) and side view (e-h) of the adsorption structures of CH_2CHCH_2* on Pt (111), Pt_3Sn (111), Pt_1Sn_1 (110) and Pt_2Sn_3 (110). Pt: blue, Sn: grey, C: black, H: white

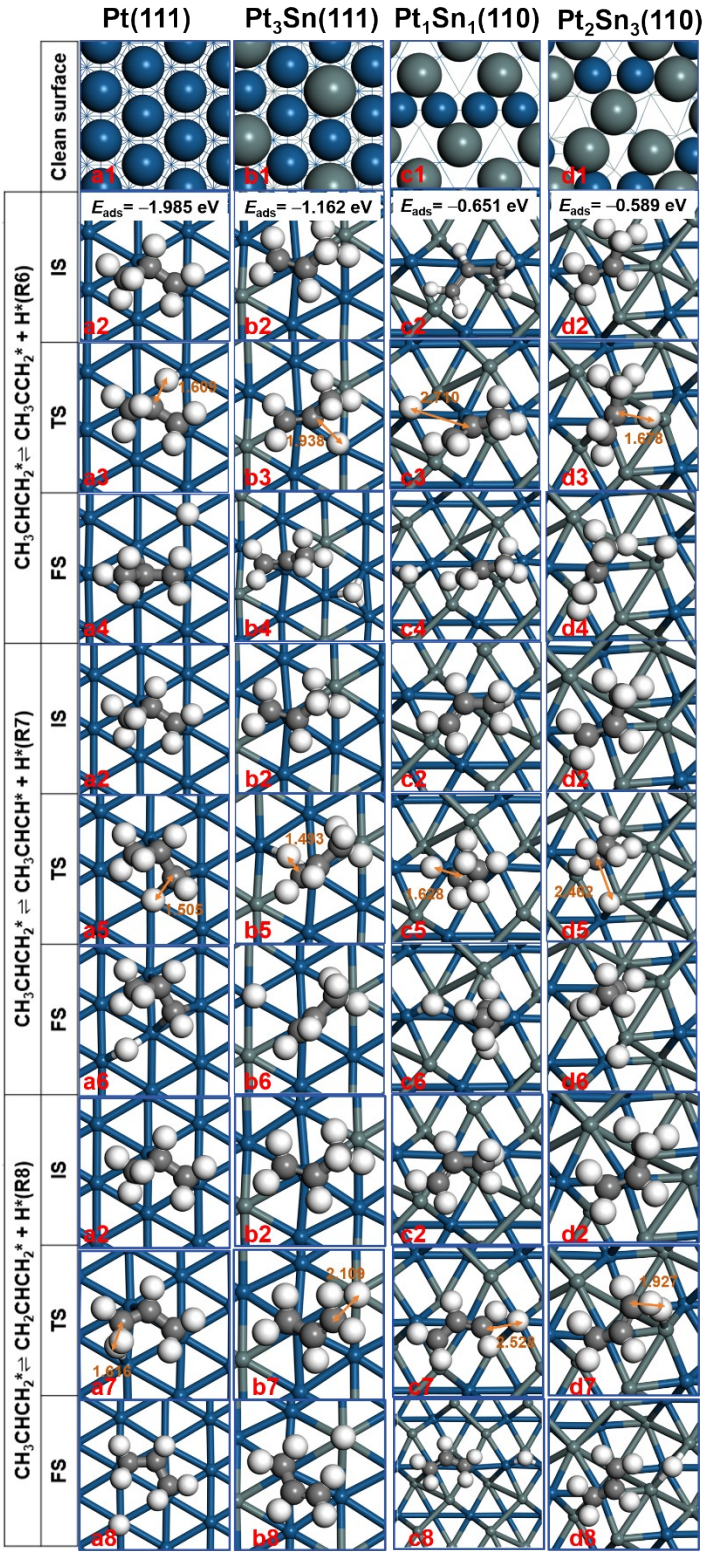

Figure S12. Top view of the optimized structures of Pt(111) (a1-a8), $Pt_3Sn(111)$ (b1-b8), $Pt_1Sn_1(110)$ (c1-c8) and $Pt_2Sn_3(110)$ (d1-d8). Initial states (IS), the corresponding transition states (TS) and final states (FS) of R6-R8 on these catalysts, along with the adsorption energies (E_{ads}). Pt: blue, Sn: grey, C:black, H:white

Table S4. Most stable adsorption sites and adsorption energies of the intermediates in the PDH reaction on the Pt (111), Pt_3Sn (111), Pt_1Sn_1 (110) and Pt_2Sn_3 (110). (Unit: eV) ([a] Adsorbed specie has no obvious bonding with the layer.)

species	Pt（111）		Pt_3Sn(111)		Pt_1Sn_1(110)		Pt_2Sn_3(110)	
	Site	E_{ads}	Site	E_{ads}	Site	E_{ads}	Site	E_{ads}
C_3H_8	--	–0.654	--	–0.414	--	–0.460	--	–0.261
$CH_3CH_2CH_2$	Pt-top	–2.651	Pt-top	–1.775	Sn-top	–1.700	Sn-top	–2.226
CH_3CHCH_3	Pt-top	–2.536	Pt-top	–1.643	Sn-top	–1.543	Sn-top	–1.996
C_3H_6	Pt-Pt bridge	–1.985	Pt-top	–1.162	--	–0.651	Pt-top	–0.589
CH_3CCH_2	fcc	–4.159	Pt-top	–2.852	Pt-top	–2.159	Pt-top	–2.316
CH_3CHCH	fcc	–4.064	Pt-Pt bridge	–3.085	Pt-top	–2.297	Pt-top	–2.318
CH_2CHCH_2	Pt-top	–2.911	Pt-top	–2.797	Pt-Pt bridge	–1.645	Pt-Pt bridge	–1.917

7. Determination of the effective barriers

Table S5. The states of TDTS and TDI, the energies of TDTS and TDI, and the calculated E_a^{eff} of two pathways over Pt (111), Pt_3Sn (111), Pt_1Sn_1 (110) and Pt_2Sn_3 (110) (see Figure 6)

	Pt(111)	Pt_3Sn(111)	Pt_1Sn_1(110)	Pt_2Sn_3(110)
TDTS	TS2	TS2	TS2	TS2
E_{TDTS}/eV	0.071	0.553	1.352	1.406
TDI	CH_3CHCH_3*+H*	$CH_3CH_2CH_2$*+H*	C_3H_8*	C_3H_8*
E_{TDI}/eV	–1.021	–0.444	–0.460	–0.261
E_a^{eff}	1.092	0.997	1.812	1.667

The effective barrier is calculated and the TOF value is obtained through eq 7.

Table S6. Energy barriers for PDH reactions on Pt (111), Pt_3Sn (111), Pt_1Sn_1 (110) and Pt_2Sn_3 (110) (Unit: eV).

	Reaction	Pt	Pt_3Sn	Pt_1Sn_1	Pt_2Sn_3
R1	$C_3H_8(g) + * \rightleftharpoons C_3H_8^*$	--	--	--	--
R2	$C_3H_8^* + * \rightleftharpoons CH_3CH_2CH_2^* + H^*$	1.206	0.628	1.522	1.248
R3	$C_3H_8^* + * \rightleftharpoons CH_3CHCH_3^* + H^*$	0.453	0.521	0.869	0.829
R4	$CH_3CH_2CH_2^* + * \rightleftharpoons C_3H_6^* + H^*$	0.405	0.784	1.452	1.301
R5	$CH_3CHCH_3^* + * \rightleftharpoons C_3H_6^* + H^*$	0.535	1.404	1.407	0.877
R6	$C_3H_6^* + * \rightleftharpoons CH_3CCH_2^* + H^*$	1.092	1.807	1.431	2.177
R7	$C_3H_6^* + * \rightleftharpoons CH_3CHCH^* + H^*$	0.592	0.978	1.019	1.563
R8	$C_3H_6^* + * \rightleftharpoons CH_2CHCH_2^* + H^*$	0.860	1.921	1.794	1.645
R9	$C_3H_8^* + * \rightleftharpoons CH_3CH_2^* + CH_3^*$	1.863	2.733	3.504	3.745
R10	$CH_3CH_2CH_2^* + * \rightleftharpoons CH_2^* + CH_2CH_3^*$	2.063	2.494	2.916	2.633
R11	$CH_3CHCH_3^* + * \rightleftharpoons CH_3^* + CH_3CH^*$	2.469	2.515	3.168	2.449

R12	$C_3H_6^* + * \rightleftharpoons CH_2CH^* + CH_3^*$	2.347	3.109	2.851	2.908

Table S7. Differences in energy barriers for deep dehydrogenation and desorption of propylene on Pt (111), Pt_3Sn (111), Pt_1Sn_1 (110) and Pt_2Sn_3 (110). (Unit :eV)

		Pt(111)	Pt_3Sn(111)	Pt_1Sn_1(110)	Pt_2Sn_3(110)
R6	$E_{a,dehydrogenation}$	1.092	1.807	1.431	2.177
$C_3H_6^* + * \rightleftharpoons$	$E_{desorption}$	1.985	1.162	0.651	0.598
$CH_3CCH_2^* + H^*$	E_{diff}	–0.893	0.645	0.780	1.579
R7	$E_{a,dehydrogenation}$	0.592	1.278	1.019	1.563
$C_3H_6^* + * \rightleftharpoons$	$E_{desorption}$	1.985	1.162	0.651	0.598
$CH_3CHCH^*+H^*$	E_{diff}	–1.393	0.116	0.368	0.965
R8	$E_{a,dehydrogenation}$	0.860	1.921	1.794	1.645
$C_3H_6^* + * \rightleftharpoons$	$E_{desorption}$	1.985	1.162	0.651	0.598
$CH_2CHCH_2^*+H^*$	E_{diff}	–1.125	0.759	1.143	1.047

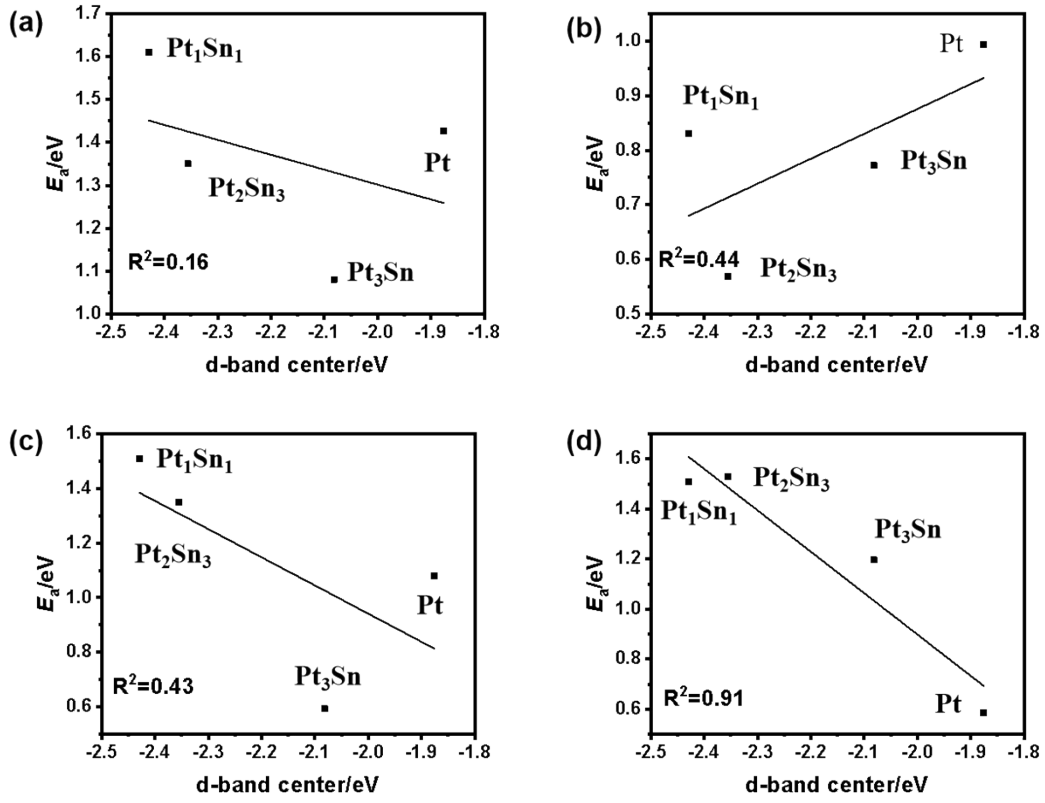

Figure S13. The propane adsorption energy and the (R2-R4) activation energies (E_a) of the three main reactions vs d-band centers.

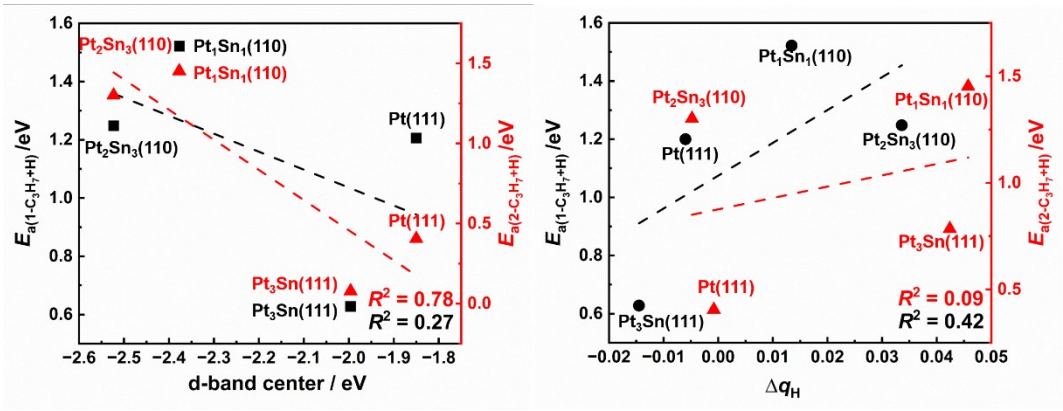

Figure S14. (a) The activation energy for the 1-propyl and 2-propyl pathways against the d-band center of Pt(111), Pt_3Sn_1(111), Pt_1Sn_1(110), and Pt_2Sn_3(110) surfaces. (b) The activation energy for the 1-propyl and 2-propyl pathways against the charge transfer of hydrogen atoms.

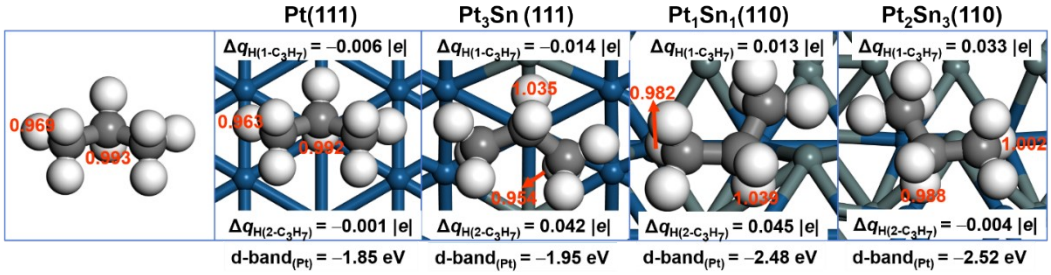

Figure S15. Bader charge analysis and d-band center of adsorption Pt site on Pt(111), Pt_3Sn(111), Pt_1Sn_1(110), and Pt_2Sn_3(110).

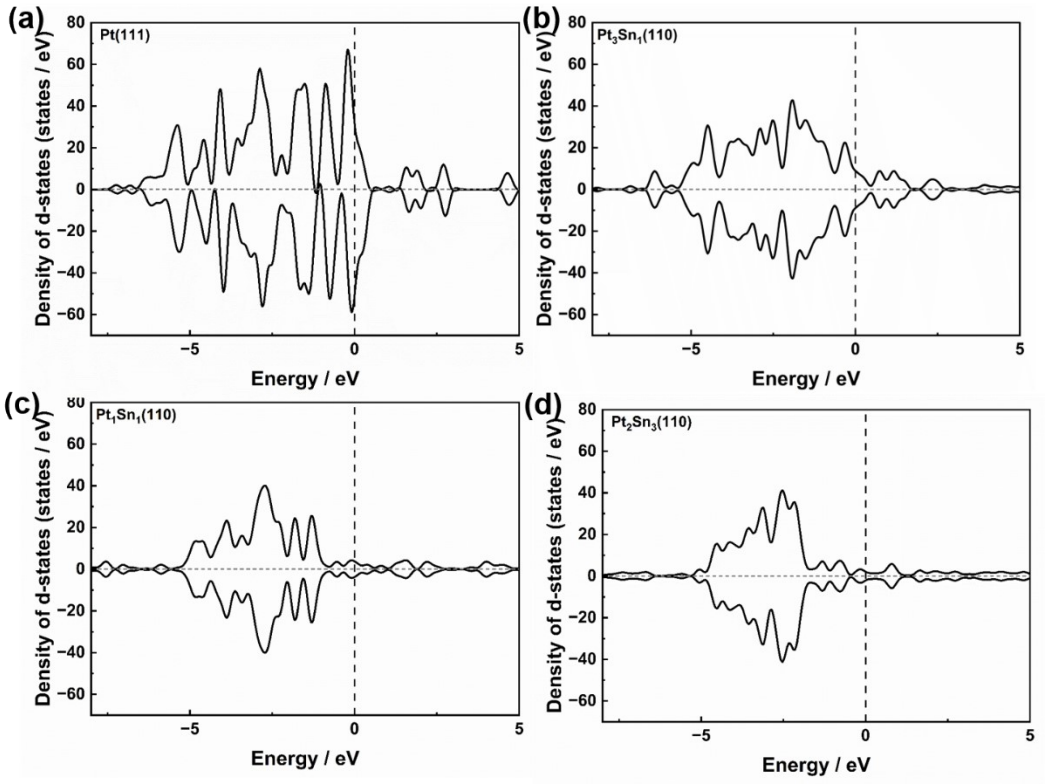

Figure S16. The Projected DOS of d-band of Pt atoms on the surface of Pt and PtSn catalysts.

Table S8. The surface generalized coordination numbers ($\overline{CN}$) of Pt (111), Pt_3Sn (111), Pt_1Sn_1 (110) and Pt_2Sn_3 (110) surfaces.

	Pt (111)	Pt_3Sn (111)	Pt_1Sn_1 (110)	Pt_2Sn_3 (110)
$\overline{CN}$	7.5	6.58	4.25	4.125

Table S9. The surface roughness (*R*) of Pt (111), Pt_3Sn (111), Pt_1Sn_1 (110) and Pt_2Sn_3 (110) surfaces.

	Pt (111)	Pt_3Sn (111)	Pt_1Sn_1 (110)	Pt_2Sn_3 (110)
$R/10^{-3}$ Å	3.572	10.522	6.986	8.858

Table S10. Comparison of adsorption energy and dehydrogenation energy barriers of propylene before and after single hydrogen atom adsorption(Unit :eV).

Species	Pt(111)		Pt_3Sn(111)		Pt_1Sn_1(110)		Pt_2Sn_3(110)	
	E_{ads}	E_a	E_{ads}	E_a	E_{ads}	E_a	E_{ads}	E_a
C_3H_6	–1.213	0.943	–0.541	1.919	–0.187	1.993	–0.190	1.471
C_3H_6+H	–1.195	1.209	–0.360	2.062	–0.071	2.057	–0.131	1.479